

## The Jets of Quasars 3C 345 and 1803+784

L. I. Matveenko

*Space Research Institute, Profsojuznaja 84/32, Moscow 117810 Russia,*  
*e-mail: lmatveen@mx.iki.rssi.ru*

A. I. Witzel

*Max-Planck-Institut für Radioastronomie, Auf dem Hügel 69, D-53121*  
*Bonn, Germany, e-mail: p0103wzl@mpifr-bonn.mpg.de*

**Abstract.** We have studied the structures of AGN objects 3C 345 and 1803+784. The objects have one sided jets with conic helix structure, determining step and diameter of the helix. The jets are surrounded by cocoon - thermal plasma, the transparency of which determines low frequency variability and absorption of the core emission.

Quasar 3C 345 ( $z=0.595$ ) and Bl Lac 1803+784 ( $z=0.68$ ) are classical AGN objects. The distances of them are 2500 and 2700 Mpc; 1 mas is equal  $\sim 4$  and  $\sim 5$  pc accordingly. The optical and radio properties are identical and structures are typical for AGN objects: core and one side jet. The core emission dominates at short radio wavelengths. The activity in the nucleus is accompanied by strong outbursts of radio emission. These outbursts appear first, and are strongest, at mm-cm wavelengths, and propagate to low frequencies while decreasing in amplitude. The low frequency variability implies a brightness temperature of the emission region  $T_b \sim 10^{16}$  K, or much greater than the limit of inverse Compton scattering -  $10^{12}$  K (Kellermann & Pauliny-Toth 1969). The outbursts are caused by knots - clouds of relativistic plasma. The apparent motions of the knots exceed the light velocity (Cohen et al. 1976). Formation of the jet is a result of the core activity. We studied the fine structure of AGN 3C 345 and 1803+784.

The low-frequency variability of 3C 345 (Padrielli et al. 1982) has the character of "negative" outbursts with a typical time-scale of one year. The low frequency variations are anti-correlated with high and uncorrelated for nearby quasars. In 1981 - 1983 activity was accompanied by strong outbursts in the frequency band 8 - 89.6 GHz (Bregman et al. 1986). An outburst 1981.6 lasted about half a year. Its spectrum had a low frequency cut off and a spectral index  $\alpha \geq 2.6$  at  $f \leq 4.8$  GHz. The spectrum of the brightest compact component had  $\alpha \geq 3$  at low frequencies. That suggests absorption of the synchrotron emission by an ionized medium. Optical depth of the medium was big even at 4.8 GHz, (Matveenko et al. 1996).

An analysis of fine structure of 3C 345 (Zensus 1991; Baath et al. 1992; Krichbaum et al. 1993; Unwin et al. 1992; Matveenko et al. 1996) showed that at 1983.0-1990.5 knots are injected inside  $\sim 60^\circ$  cone, central axis of which has P.A.  $\sim -105^\circ$ . The knots move along conical spirals. The period and

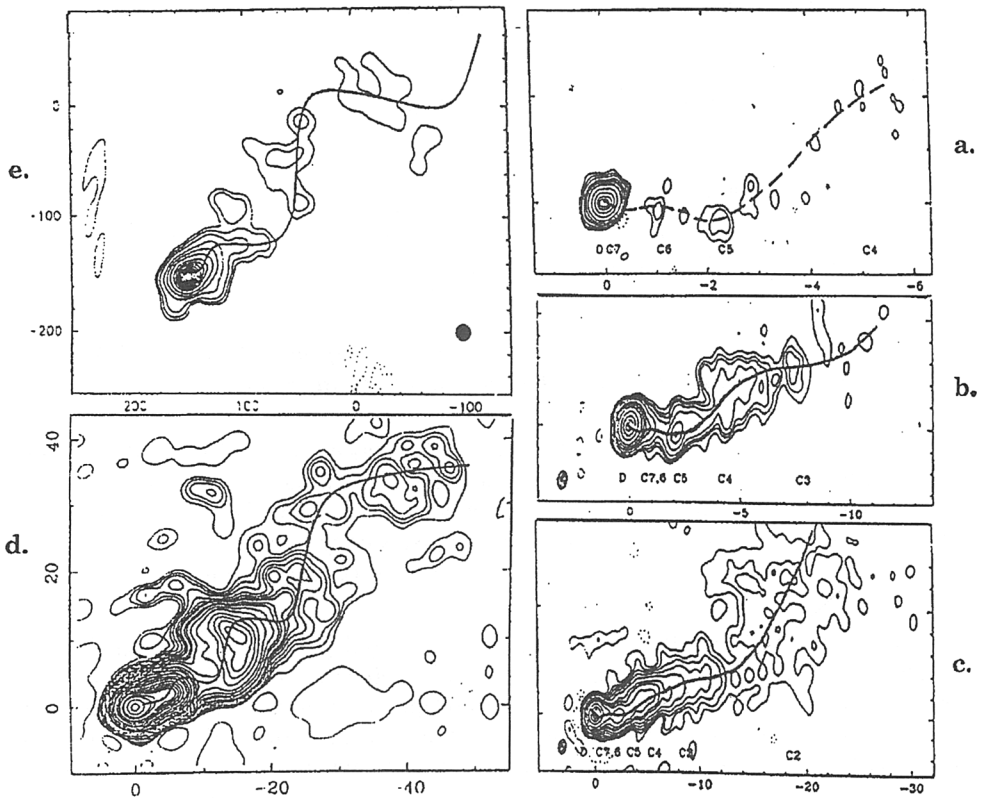


Figure 1. Images of 3C 345 at frequencies: a. 22 GHz; b. 8.4 GHz; c. 5.0 GHz (Zensus 1990); d. 1.6 GHz (Rantakuro et al. 1992); e. 0.6 GHz (Matveenko et al. 1996).

diameter of the spiral increases practically proportional to distance from the core. The direction of ejection of the knots repeated after  $\sim 7$  years. It is proposed precession period  $\sim 7$  years and the angle  $\sim 30^\circ$ .

The jet structure is a conical spiral too, Fig 1. Diameter of the spiral increases with distance  $\sim 0.55 \cdot R^{0.9}$  and step  $T = 0.15 \cdot R$  until  $R = 200$  mas, then  $T = 4.6 \cdot R^{0.4}$ . Increasing of the diameter and the step proportional to  $R$  proposes movement of relativistic plasma flow with constant velocity. A rotating flow of relativistic plasma generates a magnetic field and self-focuses in a thin stream. Velocity of rotation is determined by injector - accretion disk. The rotation axis precesses and twists the jet around the central direction forming spiral structure, which corresponds to theoretical models (Begelman et al. 1984; Lovelace et al. 1991). The twisted velocity is equal to precession velocity. The knots are moving along a magnetic tube as a stream of relativistic plasma.

The jet axis of 3C 345 is curved, orientation of it is changed from  $-105^\circ$  to  $\sim -30^\circ$  at distance  $3''$  (Browne et al. 1982). A curvature of the axis can be due to long-term precession of the rotation axis of the accretion disk. The precession angle is  $\geq 75^\circ$ .

One of the problems for studies of fine structure is the identification of components. Positions of the compact components change with time and frequency. At the high radio frequencies a reference feature is the core - the brightest compact component. However peculiar structure of the jet has features transverse to the jet axis located at  $\sim 5$ ,  $\sim 5$ ,  $\sim 30$  mas from the core. Locations are fairly stable and have smaller frequency dependence (Readhead et al. 1978; Biretta et al. 1986; Matveenko et al. 1992; Rantakyro et al. 1992; Unwin et al. 1992). We identified position of the core at  $\lambda 49\text{cm}$  with the compact component located at 16 mas, P.A. =  $95^\circ$ . Visible brightness temperature of the core is  $T_b \leq 0.003 \cdot T_{\text{peak}}$  or  $\geq 300$  times smaller than at high frequencies that corresponds to absorption at 49 cm. At 6 cm absorption will be  $\leq 4$  times.

The brightest part of the 3C 345 jet has size  $\sim 5$  mas at low frequencies, Fig. 1. At the period 1983.9 - 1990.8 at wavelength  $\lambda = 49\text{cm}$  flux density and angular size increased  $\sim 2$  times, but the brightness temperature did not change significantly and was  $T_b = 0.6 \cdot 10^{12}$  K. Emission at millimetre wavelengths and UV decreased by a factor of  $\sim 2$  during the same time. A stable brightness temperature of the region, limitation of  $T_b \leq 10^{12}$  K, cut off steep spectrum and changed size of the emission region confirm the absorption nature of low frequency variability.

Ionized gas surrounding the core of AGN objects radiates emission lines. Electron density of the narrow line medium is  $10^{4-6}\text{cm}^{-3}$  and dimension is  $\sim 10^{20}$  cm or  $\sim 8$  mas for 3C 345. Absorption of the ionized medium -  $e^-$  - is determined by optical depth:

$$\tau = 0.08 \cdot T_e^{-1.35} (1+z)^{-2.1} f^{-2.1} \int N_e^2 dl \quad (15)$$

The optical depth at  $\lambda 49\text{cm}$  is  $16 \cdot 10^{-8} ME$ . A flow of relativistic plasma - jet is surrounded by thermal plasma in the form of a cocoon. The density of thermal electrons of recombination time and time of low frequency variability  $\sim 1$  yr is  $N_e \sim 10^5\text{cm}^{-3}$ . The pressure in the jet varies with density as  $P_j \sim (R_o/R)^2$  and  $N_{rme} \sim (R_{rmo}/R)^2$  (Begelman et al. 1984). The wall thickness increases with distance from the nucleus. The optical depth of the wall is  $7 \cdot 0 R^{-3}$ . Optical depth of the injector region  $\tau \sim 6$  at  $\lambda 49\text{cm}$  and thickness of the cocoon wall will be  $l \sim 10^{-3} pc$ .

Bright components are distributed in the nearest part of the 6 mas jet region. Transparency of the cocoon wall changes with distance and time. At high frequencies, the screen is transparent. However, it changes polarization. At 1980-1993 changes of emission were accompanied by variations of the polarization at  $\lambda 6$  cm (Brown et al. 1994). The polarized radiation increased simultaneously with total until a definite level after which was observed anti-correlation. Polarized emission  $\lambda = 6$  cm increases with distance from the core and reaches a maximum at distance  $\sim 4.5\text{mas}$ . The rotation measured at  $\lambda = 18-21$  cm, (beam size  $\sim 5''$ ) is  $RM \sim 28\text{rad m}^{-2}$  and the degree of polarization  $\sim 4\%$  (Rudnick et al. 1983). The 18 and 6 cm maximum of polarized emission arises from the same region. The degree of polarization depends on bandwidth and RM. Increasing of  $N_{rme}$  increases RM and decreases polarized emission (Matveenko et al. 1996). The polarization position angle, corrected for Faraday rotation, is  $\sim 70^\circ$  and is parallel to the jet. The rotation measure

$RM \sim (R_o/R)^3$  and equals  $3500 \text{ rad m}^{-2}$  at the core region and magnetic field  $B_{\parallel} \sim 0.1 \text{ mG}$ .

Brightness temperature of the nearest part of the jet ( $R \leq 2 \text{ mas}$ ) is  $T_b \sim 10^{12}$  K (high frequencies) and corresponds to the kinetic temperature of relativistic plasma. At distance  $R \leq 25 \text{ mas}$   $T_{rmb} \sim 0.5 \cdot 10^{12}$  K (low frequencies). At  $R \sim 50 \text{ mas}$  optical depth of the emission region is not big and  $T_b \sim 10^9$  K and decreases until  $\sim 10^7$  K at  $1''$ - $4''$  distances. Spectral index (along spiral with the angular resolution  $1 \text{ mas}$ ) of the nearest part of the spiral ( $2 \leq R \leq 10 \text{ mas}$ ) is equal  $\alpha = -1.0 \pm 0.3$  at ( $\lambda = 1.3$ - $3.6 \text{ cm}$ ) and  $\alpha = -0.5 \pm 0.3$ , ( $\lambda = 3.6$ - $6 \text{ cm}$ ). Part of the jet at  $10$ - $50 \text{ mas}$  distance has spectral index  $\alpha = -0.9 \pm 0.3$  ( $\lambda = 18$ - $49 \text{ cm}$ ). Spectral index increases from a  $\alpha = -0.8$  at distance  $1''$  to  $\alpha = -1.5$  at  $4''$  from the core.

Low frequency variability of 1803+784 has a typical time  $1.5 \text{ yr}$  just as at high frequencies is a few days. We studied structure of object 1803+784 at  $18 \text{ cm}$  with global VLBI network 29 May 1993 with dynamic range  $\leq -30 \text{ dB}$ . Brightness distribution ( $0.3 \text{ mas}$ ) is located in two groups at distance  $25 \text{ mas}$  one from the other inside a  $23^\circ$  cone. The axis of the cone is curve, Fig. 2. Position angle changes with distance  $R$ ,  $PA = -(90 + 1.5 \cdot R)^\circ$ . The injector region has jet like structure and consists of few components, peak is  $F = 3.54 \text{ Jy/beam}$ . The brightness distribution with averaging beam  $2 \text{ mas}$  is shown in Fig. 2b, minimum level is  $0.07\%$  of peak. At Fig. 2c is shown strip distribution along an injector axis by a fan beam  $0.3 \cdot 3.0 \text{ mas}$ ,  $PA = -10^\circ$ . We propose that the core is located left at  $2.8$ - $3 \text{ mas}$  from the peak and has very weak brightness ( $\leq 20 \text{ dB}$ ) of the peak. The brightness increases from the core can be explained by increasing transparency of the surrounding medium. Optical depth of the medium changes approximately linearly and equals:

$$\tau = \tau_o(1 - R/R_o), \quad (16)$$

where  $\tau_o = 5.5$  the optical depth in the injector region and  $R_o = 3 \text{ mas}$  is core location relative to the bright peak.

The electron density of the thermal plasma in the region with maximum emission at  $18 \text{ cm}$ ,  $R \sim 3 \text{ mas}$  of the core, can be calculated the time of recombination and low frequency variability  $N_e \geq 0.5 \cdot 10^5 \text{ cm}^{-3}$ . Thickness of the screen is  $l \sim 10^{-2} \text{ pc}$ . Changing optical depth at  $20$ – $30\%$  explains low frequency variability.

The compact components are located from  $0.1$  to  $25 \text{ mas}$  of the injector. Ejections of the compact components is direction  $PA \sim -(68 - 110)^\circ$ . The cone of ejected components is  $\sim 40^\circ$  and direction of the cone axis is  $-90^\circ$ . The components are moving along a conical spiral trajectory (Krichbaum et al. 1993). Angle of the cone is  $34^\circ$  and practically corresponds to the cone of  $18 \text{ cm}$  structure. Diameter of the spiral increases with distance of  $\sim 0.6 \cdot R$  and period  $T \sim R$ .

Polarized emission of 1803+784 at  $18$ - $21 \text{ cm}$  is  $P = 3.9\%$ ,  $PA = -129^\circ$  and rotation measure  $RM = -62 \text{ rad m}^{-2}$ . This position angle is different from the jet orientation  $\sim -30^\circ$  (Wrobel et al. 1987). Sign and value of RM is different from the nearest sources  $RM \sim 20 \text{ rad m}^{-2}$ , which corresponds to RM of Galaxy. In this case 1803+784  $RM \sim -80 \text{ rad m}^{-2}$ . This value of rotation measure corresponds to the brightest region located at  $3 \text{ mas}$  from the injector. At  $3.6$

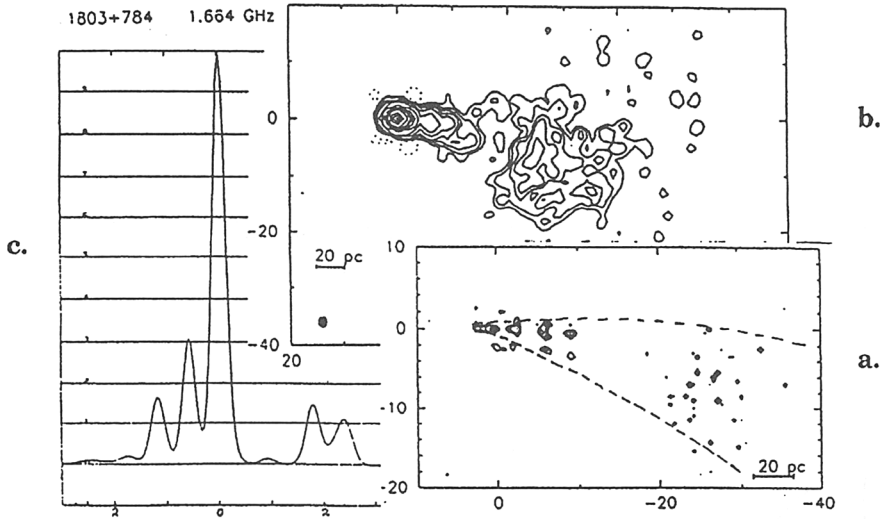


Figure 2. Images of 1803+784 at 1.6 GHz, beam size: a. 0.3 mas; b. 2 mas; c. 0.3\*3.0 mas PA=-10°

cm the main polarized emission is determined by the core region,  $P = (15-20)\%$  and position angle is  $PA = 90^\circ$ , that corresponds to orientation of the jet.

The changing of the polarization level can be determined by changing optical depth of emission regions. A Thin source has  $P_o \leq 70\%$  and orientation of E perpendicular to the magnetic field. For thick one  $P_o \leq 10\%$  and E is parallel to B. At 3.6 cm  $P = 20\%$ ,  $T_b \leq 10^{12}$  K and optical depth probably thin or practically thin, E would be perpendicular to B. At 18 cm the emission region is thick,  $T_b \sim 10^{12}$  K, E would be parallel to magnetic field B. The parameters of cocoon wall at  $\lambda 18cm$ ,  $R=2.8$  mas:  $N_e \sim 10^5$  and  $l = 10^{-2}$  pc. Rotation measure is:

$$RM = 8.1 \cdot 10^5 N_e B l, \text{ rad/m}^2.$$

For  $RM = 80$  and regular magnetic field in observer's direction (perpendicular to jet axes) is  $B_{||} \sim 0.1 \mu G$ .

At  $\lambda 18cm$  are two regions located at distance  $\sim 704mas$ . Orientation of the polarization is perpendicular (S. Aaron, private information). Perhaps changes  $\sim 1.5rad$  is determined by changing of  $RM(R)$  at the relative distance  $\Delta R = 4mas$  and  $\Delta RM = 46rad/m^2$ . Rotation measure in region of the maximum emission  $RM \sim -80rad/m^2$  and  $RM = -34rad/m^2$  at 4 mas.

The jets of the 3C 345 and 1803+784 have conical spiral structure, diameter and step of which are  $\sim R$ . Axis of the jets have helical form. Brightness temperature of the injector  $T_b \leq 7 \times 10^{12}$  K.

The jet is surrounded by a thermal plasma cocoon. Electron density of the cocoon is  $N_e 10^5 cm^{-3}$ , thickness of the wall  $\leq 10^{-2}$ .

Low frequency variability is determined by changing transparency of the cocoon.

**Acknowledgments.** LM is grateful to the IAU Colloquium organizers and INTAS for hospitality and financial support.

## References

- Baath, L. B., et al. 1992, *A&A*, 257, 31.  
Begelman, M. C., et al. 1984. *Rev. Mod. Phys.*, 56, 255.  
Biretta, J. A., et al. 1986. *apj.*, 308, 93.  
Bregman, J. N., et al. 1986, *apj.*, 301, 708.  
Browne, I. W. A., et al. 1982, *mnras.*, 198, 673.  
Brown, L. F., et al. 1994. *ApJ*, 437, 108.  
Cohen, M. H., et al. 1976. *ApJ*, 206, L1.  
Kellermann, K. I., et al. 1969. *ApJ*, 155, L31.  
Krichbaum, T. P., et al. 1993. *A&A*, 275, 375.  
Lovelace, R. V., et al. 1991, *ApJ*, 379, 695.  
Matveenko, L. I., et al. 1992. *Pisma Astron. Zh.*, 18, 379.  
Matveenko, L. I., et al. 1996. *A&A*, 312, 738.  
Padielli, L., 1982, *Proc. NRAO Workshop*, W.D. Cotton and S.R. Spangler(eds.), p.1.  
Rantakyrö, F. T., et al. 1992. *A&A*, 259, 8.  
Readhead, A. C. S., 1978. *Nature*, 276, 768.  
Rudnick, L., et al. 1983. *apj*, 88, 518.  
Unwin, S. C., et al. 1992, *apj*, 398, 74.  
Wrobel, J. M. et al. 1987, *IAU Symposium No 129*, 165.  
Zensus, J. A. 1991, "Extragalactic Radio Sources - From Beam to Jets", J. Roland, H. Sol, and G. Pelletier (eds.), "Cambridge University press", p.154.